Theoret. Chim. Acta (Berl.) 49, 295–307 (1978)

THEORETICA CHIMICA ACTA

Orbit–Orbit Interaction between Iron(III) Kramers Doublet and Porphyrin π-Orbitals Studied by Magnetic Circular Dichroism of Low-Spin Ferriheme Compounds

Alexander P. Mineyev and Yurii A. Sharonov

Institute of Molecular Biology, Academy of Sciences, Moscow 117 312, U.S.S.R.

To explain the temperature dependence (as $1/T$) of the magnetic circular dichroism (MCD) observed in the $\pi-\pi^*$ bands of low-spin ferriheme compounds, we present the theoretical treatment based on the exchange-type $\pi-d$ interaction. The four-fold degeneracy of both B and Q excited states ($3d$-iron(III) Kramers doublet × porphyrin orbital $E(\pi)$-doublet) is to be partially lifted due to intraconfiguration interaction. The transitions between the ground and excited Kramers doublets give rise to MCD of two types. Instead of temperature independent A-type effect usually observed in both B and Q bands of metal porphyrin MCD spectra, there will be two A-type effects of the same sign and two temperature dependent C-type effects of opposite signs. The values of energy gaps between orbit–orbit split sublevels are predicted to be generally different for the visible Q- and the near UV B-band. The previous theoretical models [3, 4] are discussed and some experimental evidence in favour of our interpretation are presented.

Key words: Magnetic circular dichroism (MCD) – Low-spin heme compounds – Kramers doublet

1. Introduction

Magnetic circular dichroism (MCD) is known to be of three physically distinguished types, which arise respectively from the Zeeman splitting of either ground and/or excited states (A-type effects), the mixing by external magnetic field of different unperturbed states (B-type effects), and the change in population of sublevels of the ground state, as a result of its Zeeman splitting (C-type effects). The A- and B-type effects are temperature independent, while the C-type ones depend on the temperature according to Boltzmann's law, i.e. as $1/T$ when Zeeman splitting is much less than a sample temperature. On the other hand, the

0048-5744/78/0049/0295/$02.60

A-type effects are characterized by derivative-shaped dispersion curves, while the *B*- and *C*-type ones have the same frequency dependence, which resembles an absorption band [1].

In the most of recent papers [2–6] on the low temperature MCD of paramagnetic heme compounds the temperature-dependent MCD in $\pi-\pi^*$ bands have been found. At first sight these observations are in concordance with the above-mentioned statement about the *C*-type effects. Indeed, the non-zero iron spin must result in the Zeeman splitting of a ground state. But more careful consideration shows that the spin degeneracy alone is not sufficient to give rise to *C*-type effects [7]. It is necessary at the same time to split an excited state by some interaction, which must be correlated with spin selection rules, say, by spin–orbit coupling. However, when spin and orbital momenta are localized on different orbitals, as in $\pi\rightarrow\pi^*$ excited configurations of heme compounds, the mechanism of the splitting has to be clarified.

To our knowledge there are two interpretations concerning this question. Livshitz *et al.* [3] have supposed spin–orbit coupling of circular orbital motion of porphyrin electrons with a foreign spin located at the iron ion. Kobayashi *et al.* [4] have interpreted this splitting as a result of configuration interaction of the $\pi\rightarrow\pi^*$ state with the near infra-red $\pi\rightarrow d^*$ state.

These assumptions seem to us now to be somewhat artificial. We propose here the other theoretical explanation of the nature of this splitting. Our model is based only on the well-established data about the electronic structure of the compounds under consideration. We report also some experimental results to support our interpretation.

2. Near UV and Visible MCD of Low-Spin Iron(III) Porphyrin Complexes at Room and Low Temperatures

All metal porphyrins exhibit similar spectral properties. The absorption spectra are characterized by a weak Q band in the visible and a very strong near UV B, or Soret, band [8]. The MCD intensities of these bands vary in a wide interval because they depend also on the magnetic moments of excited Q and B bands (see for example [12]).

In the simplest explanation of these facts proposed by Simpson [10] a porphyrin ring has been regarded as a free electron circular box with 18 electrons. One-electron wave functions of such a system are proportional to $\exp(\pm im\phi)$, where m is a quantum number determining both the energy and the angular momentum of an electron. The transitions between the top filled $|\pm4\rangle$ and the lowest empty $|\pm5\rangle$ orbitals result in the excited states $Q(\pm9)$ and $B(\pm1)$. The former is rigorously forbidden in the dipole approximation (a weak absorption in real molecules) while the latter is allowed ($\Delta m=\pm1$). Moreover, using a Hund's-like rule, one can conclude the lower energy of the Q state as compared with that of the B state.

Apparently such a $D_{\infty h}$ treatment could not describe the distinctive features of any real porphyrin spectrum. Gouterman [8] has proposed the more realistic "four-orbital" model, which implies an appreciable interaction between pure configurations arising due to $a_{1u} \rightarrow e_g$ and $a_{2u} \rightarrow e_g$ transitions. The resulting quasi-forbidden Q state and strongly allowed B state are of the same E_u-symmetry and therefore give rise to the A-type effects in the MCD. The Q/B magnetic moment ratio appears to be more than unity, but unlike the Simpson's model, where it is precisely equal to 9, it may vary significantly, depending on the central metal ion, substituent peripheral groups etc. [9].

The four-orbital ideas had been supported by a great number of spectroscopic and quantum chemical studies and constitute now the theoretical ground of any investigation concerning porphyrin spectra.

Before the first low temperature MCD measurements one could believe the spectral properties of low-spin iron(III) porphyrins to be similar to those of other metal porphyrins (see for example [9]). The unusual broadening of the visible bands was not a grave reason for refinement of previous theory. This step was initiated by the finding of the temperature dependence of MCD intensities in the B band. The temperature effects have been observed first in ferricytochrome b_2 by Briat *et al.* [2].

It should be pointed out that hemeproteins (cytochromes, hemoglobin, myoglobin, catalase, peroxidase etc,) are largely used in MCD studies since their principal spectral characteristics do not differ from those of other heme complexes, moreover hemeproteins show no aggregation inherent to many porphyrins.

Later the temperature dependent MCD in B band has been revealed in other low-spin iron(III) porphyrin complexes such as ferricytochrome *c* [3], bisimidazole complexes of Fe(III) tetraphenyl- and Fe(III) octaethylporphyrin [4], ferricytochrome b_5 and ferrimyoglobin CN^- complexes [5].

The latter has been recently observed by Springall *et al.* [6] to exhibit the derivative-shaped C-type MCD in the Q band too, especially appreciable at liquid helium temperatures.

We present here the MCD and absorption spectra of peroxidase and catalase CN^- complexes (Figs. 1 and 2) recorded at room and liquid nitrogen temperatures. Possessing the spectral properties typical for all low-spin ferriheme compounds these samples were used to illustrate our theoretical interpretation.

As any low-spin ferriheme complex [2–6], catalase and peroxidase exhibit A-like effects of normal sign, i.e. a long-wavelength wing is negative. On lowering the temperature from 300 to 77°K the B-band MCD intensities show more than threefold increase. The temperature dependence of MCD *per se* is not sufficient to speak about the C-type effects because the intensity of the A-type effects is very sensitive to the temperature-induced changes in the width of the corresponding absorption band [1].

However, the absence of appreciable temperature changes in near UV absorption spectra of CN^- peroxidase (Fig. 1) and CN^- catalase (Fig. 2), jointly with nearly

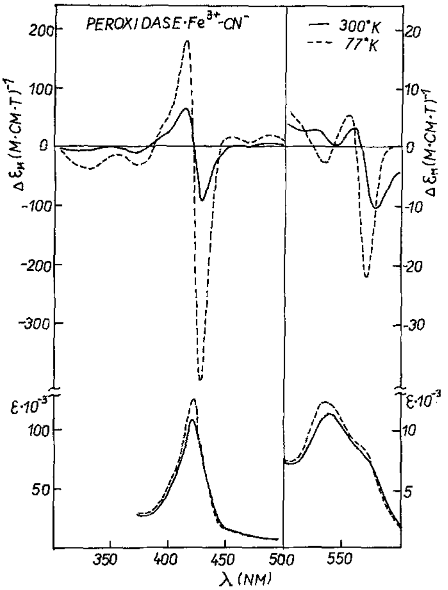

Fig. 1. Magnetic circular dichroism and absorption spectra of the cyanide complex of Fe(III)-horseradish peroxidase at room (——) and liquid nitrogen (- - -) temperatures. Protein concentration $7.7\cdot 10^{-5}$ M in near UV and $7.7\cdot 10^{-4}$ M in the visible; in an equal-volume mixture of glycerol and 0.2 M sodium phosphate buffer at pH 6.8; pathlength 2.0 mm; magnetic field 1.35 T.

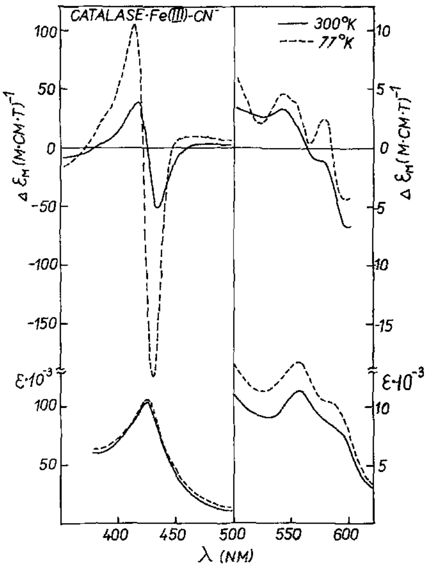

Fig. 2. Magnetic circular dichroism and absorption spectra of the cyanide complex of Fe(III)-catalase at room (——) and liquid nitrogen (- - -) temperatures. Protein concentration $3.5\cdot 10^{-5}$ M in near UV and $2.0\cdot 10^{-4}$ M in the visible (per heme); in an equal-volume mixture of glycerol and 0.2 M sodium phosphate buffer at pH 6.8; pathlength 2.0 mm; magnetic field 1.35 T

four-fold increase of MCD intensities clearly indicate the existence of *C*-type effects in B-bands of these compounds.

The situation is not so clear in the Q region. Therefore, for reliable detection of *C*-type effects in the Q band, measurements down to liquid helium temperature are required (see below).

3. Theory

To make our treatment perfectly transparent we firstly wish to report it in terms of the free electron model, and then to extend the interpretation over the square iron(III) porphyrins.

3.1. Free Electron Consideration

As already pointed out, the ground state of the 18-electrons ring will be

$$G(0)=|+4+\bar{4}-4-\bar{4}| \qquad (1)$$

In this ± 4, $\pm\bar{4}$ are the highest occupied spin orbitals with opposite spin (lower-lying orbitals are omitted).

Iron(III) d^5 system are conveniently represented by a coaxial ring with 5 electrons, since the highest incompletely filled low-spin iron(III) $d_{\pm 1}$ orbitals have the ϕ-angular part given by $\exp(\pm i\phi)$. Hence, the ground Kramers doublet of the double-ring complex may be written as follows (spin–orbit coupling has already been taken into account):

$$\begin{aligned} \mathrm{G}^+(+1) &= |+4+\bar{4}-4-\bar{4}+1+\bar{1}-1| \\ \mathrm{G}^-(-1) &= |+4+\bar{4}-4-\bar{4}-1-\bar{1}+\bar{1}| \end{aligned} \tag{2}$$

where the superscripts ± refer to the total spin and the numbers ±1 given in the parentheses indicate the total angular momentum.

Instead of the uniring spin allowed Q(±9) and B(±1) states we have now

$$\begin{aligned} \mathrm{Q}^+(+10) &= \{|+4+\bar{4}-4+\bar{5}+1+\bar{1}-1| - |+4+\bar{4}-\bar{4}+5+1+\bar{1}-1|\}/\sqrt{2} \\ \mathrm{Q}^-(-10) &= \{|+4-\bar{5}-4-\bar{4}-1-\bar{1}+\bar{1}| - |+\bar{4}-5-4-\bar{4}-1-\bar{1}+\bar{1}|\}/\sqrt{2} \\ \mathrm{Q}^+(-8) &= \{|+4-\bar{5}-4-\bar{4}+1+\bar{1}-1| - |+\bar{4}-5-4-\bar{4}+1+\bar{1}-1|\}/\sqrt{2} \\ \mathrm{Q}^-(+8) &= \{|+4+\bar{4}-4+\bar{5}-1-\bar{1}+\bar{1}| - |+4+\bar{4}-\bar{4}+5-1-\bar{1}+\bar{1}|\}/\sqrt{2} \end{aligned} \tag{3}$$

and

$$\begin{aligned} \mathrm{B}^+(+2) &= \{|+4+\bar{5}-4-\bar{4}+1+\bar{1}-1| - |+\bar{4}+5-4-\bar{4}+1+\bar{1}-1|\}/\sqrt{2} \\ \mathrm{B}^-(-2) &= \{|+4+\bar{4}-4-\bar{5}-1-\bar{1}+\bar{1}| - |+4+\bar{4}-\bar{4}-5-1-\bar{1}+\bar{1}|\}/\sqrt{2} \\ \mathrm{B}^+(0) &= \{|+4+\bar{4}-4-\bar{5}+1+\bar{1}-1| - |+4+\bar{4}-\bar{4}-5+1+\bar{1}-1|\}/\sqrt{2} \\ \mathrm{B}^-(0) &= \{|+4+\bar{5}-4-\bar{4}-1-\bar{1}+\bar{1}| - |+\bar{4}+5-4-\bar{4}-1-\bar{1}+\bar{1}|\}/\sqrt{2} \end{aligned} \tag{4}$$

respectively.

The B-states, as they are given by Eq. (4), have been considered by Kobayashi *et al.* [4] to demonstrate how the splitting caused by configuration interaction with the charge transfer $\pi \rightarrow d^*$ ($4 \rightarrow 1$) state, could arise. However, it is sufficient to take into account the intraconfiguration interaction only to get the desired splitting. Indeed, both B- and Q-states have the four-fold degeneracy until there is no interaction between rings. (Just as uniring Q(±9) and B(±1) states are at the same energy level in the absence of electron repulsion.)

The energy gaps resulted from such an inter-ring exchange interaction are given below

$$\begin{aligned} \Delta \mathrm{Q} &\equiv E[\mathrm{Q}^\pm(\pm 10)] - E[\mathrm{Q}^\pm(\pm 8)] = \{(K_{41}-K_{4-1}) + (K_{51}-K_{5-1})\}/2 \\ \Delta \mathrm{B} &\equiv E[\mathrm{B}^\pm(\pm 2)] - E[\mathrm{B}^\pm(0)] = \{(K_{41}-K_{4-1}) - (K_{51}-K_{5-1})\}/2 \end{aligned} \tag{5}$$

where K_{ij} is the exchange integral defined as follows

$$K_{ij} \equiv \langle ij \mid ji \rangle = \int i^*(1) j^*(2) (e^2/r_{12}) j(1) i(2)\, \mathrm{d}\tau_{12} \tag{6}$$

According to Kramers theorem the electrostatic interaction can not lift the Kramers degeneracy and thus each of the states $\mathrm{Q}^\pm(\pm 10)$, $\mathrm{Q}^\pm(\pm 8)$, $\mathrm{B}^\pm(\pm 2)$, $\mathrm{B}^\pm(0)$ remains doubly degenerate representing an excited Kramers doublet.

One can now predict the peculiarities arising in the MCD spectra of the double-rings complex as compared with the simple circular box. When there is only one

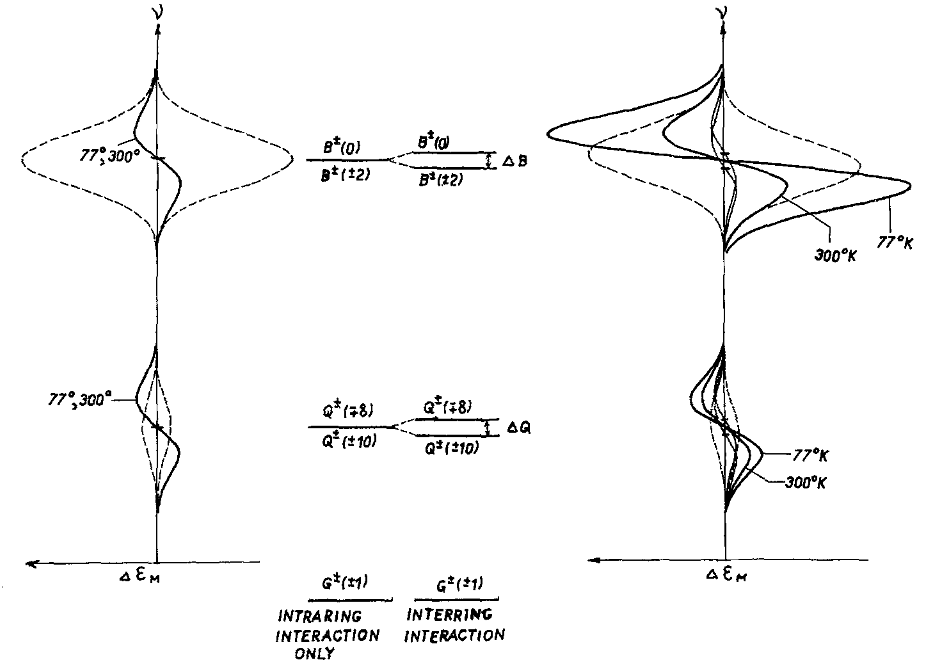

Fig. 3. The energy level diagram and the theoretical MCD of the double-ring complex in the absence (left panel) and in the presence (right panel) of inter-ring interaction. The *C*-type effects at room temperature (dashed line), *A*-type effects (fine line) and resulting MCD curves (thick line) are calculated assuming Gaussian shape of bands and $\Delta Q = \Delta B$. *C*/*A*-ratios for B band are 9 times as great as those for the Q band (see text)

ring with 18 electrons the MCD effects are obviously attributed to the orbital angular momentum of excited states. The transitions $G(0) \rightarrow B(\pm 1)$ and $G(0) \rightarrow Q(\pm 9)$ give rise to two *A*-type effects of the same sign [9].[1] If now the coaxial ring with 5 electrons has been placed the overall ground state becomes degenerate. The external magnetic field splits the ground Kramers doublet so that $G^-(-1)$ is more populated than $G^+(+1)$ and therefore transitions from $G^-(-1)$ will be more intensive than those from $G^+(+1)$ especially at reduced temperatures. But no changes in MCD should be expected unless two rings are independent because excitation of interest occurs inside the outer ring, while the Zeeman splitting of the ground state takes place on the inner one. More formally, the two *C*-type effects of opposite sign will be located in the same position annihilating each other (see Fig. 3, left panel).

As it follows from Eq. (5) the B and Q quartets are split owing to inter-ring exchange interaction. This results in mutual shifts of opposite *C*-effects, and some temperature dependence of MCD is observed. At the same time the transitions $G^\pm(\pm 1) \rightarrow B^\pm(0)$, $B^\pm(\pm 2)$, $Q^\pm(\pm 8)$, $Q^\pm(\pm 10)$ give rise to the *A*-type effects as well. Therefore the overall MCD will be the sum of these *C*- and *A*-type effects.

---

[1] This means that both in B- and in Q-bands the left-circularly polarized light will be absorbed at higher frequencies than right one because of Zeeman splitting and selection rules are determined by the same quantum number in Simpson's model.

To predict the sign of resulting MCD bands it is necessary to know the signs of ΔQ and ΔB of Eq. (5). If the Hund's-like rule is acceptable, one can imagine the MCD spectrum as shown in Fig. 3 (right panel), provided uniring MCD looks like that shown on the left panel of Fig. 3.

It should be noted that the spin–orbit coupling of the ground state is of great importance in such a treatment, because it correlates the circular polarization of any given transition with spin selection rules and therefore determines the sign of MCD. For example, excitations $G^-(-1) \rightarrow B^-(0)$ and $G^+(+1) \rightarrow B^+(+2)$ are left circular polarized, while $G^-(-1) \rightarrow B^-(-2)$ and $G^+(+1) \rightarrow B^+(0)$ are right circular polarized. Taking into account the higher population of $G^-(-1)$ sublevel the positive MCD will prevail at $B^{\pm}(0)$-energy and negative MCD will prevail at $B^+(\pm 2)$ energy.

Fig. 3 shows that the temperature dependence in the Q band is remarkably less than that in the B band because of the much greater C/A ratio for the B band as compared with that for the Q band. This reflects the fact that C-terms are proportional to the ground state magnetic moment, identical for both bands, while temperature-independent A-terms are proportional to the Zeeman splittings both of the ground and of the excited states. Hence, even at sufficiently low temperatures, A-terms in the MCD Q band may prevail over C-terms.

Generally, a rather simple analysis shows that when $\Gamma \gg \Delta$ (where Γ and Δ are band halfwidth and zero-field splitting respectively) the relative amplitude of temperature-dependent and independent MCD in the splitted band is given by

$$\frac{\Delta\varepsilon(C)_{\max}}{\Delta\varepsilon(A)_{\max}} = \frac{\Delta}{T} \cdot \frac{\mu_0}{\mu_e - \mu_0} \tag{7}$$

Here μ_0 and μ_e are magnetic moments of ground and excited states respectively. Decreasing of Δ and/or increasing of the μ_e will enhance the relative contribution of A-type effects. In particular, when Δ is equal to zero two C-type effects cancel each other.

So the main experimentally observable features of the low-temperature MCD spectra of low-spin iron(III) heme compounds could be qualitatively understood even in terms of the free electron model. More rigorous interpretation is presented in the next section.

3.2. Four-Orbital-Like Consideration

Gouterman's four-orbital model [8] may be briefly formulated as follows. The electronic transitions from top-filled porphyrin π-orbitals a_{1u} and a_{2u} to the lowest-lying empty e_g-orbital after configuration interaction give rise to two excited states, namely

$$\begin{aligned} B_x &= \sin\theta\{a_{1u}e_{gy}\} + \cos\theta\{a_{2u}e_{gx}\} \\ B_y &= \sin\theta\{a_{1u}e_{gx}\} - \cos\theta\{a_{2u}e_{gy}\} \\ Q_x &= \cos\theta\{a_{1u}e_{gy}\} - \sin\theta\{a_{2u}e_{gx}\} \\ Q_y &= \cos\theta\{a_{1u}e_{gx}\} + \sin\theta\{a_{2u}e_{gy}\} \end{aligned} \tag{8}$$

where θ is the mixing parameter defined by

$$\tan 2\theta = 2\langle e_{gy}a_{2u} \mid a_{1u}e_{gx}\rangle / (E\{a_{2u}e_g\} - E\{a_{1u}e_g\}) \tag{9}$$

and could be determined from the absorption spectrum provided certain assumptions have been made [8].

As to the electronic structure of the central iron(III) the numerous EPR studies show a remarkable deviation from octahedral ligand symmetry in all ferric heme compounds. Such a distortion results in the splitting of $^2T_{2g}$ sextet into three Kramers doublets. Energy gaps between them have been evaluated to be of the order of 1000 cm^{-1}. In the crystal field approximation any of these Kramers doublets is conveniently described [11] by

$$\begin{aligned} |+\rangle &= a \mid \xi\alpha\rangle - ib \mid \eta\alpha\rangle - c \mid \zeta\beta\rangle \\ |-\rangle &= -a \mid \xi\beta\rangle - ib \mid \eta\beta\rangle - c \mid \zeta\alpha\rangle \end{aligned} \tag{10}$$

where a, b, c are real constants, which could be determined in principle providing the g-values are known.

$|\xi\alpha\rangle$, $|\eta\alpha\rangle$ etc. of Eq. (10) are the $3d$-hole wave functions:

$$\begin{aligned} &|\xi\alpha\rangle \equiv |\zeta\bar{\zeta}\eta\bar{\eta}\xi| && |\xi\beta\rangle \equiv |\zeta\bar{\zeta}\eta\bar{\eta}\bar{\xi}| \\ &|\eta\alpha\rangle \equiv |\zeta\bar{\zeta}\xi\bar{\xi}\eta| && |\eta\beta\rangle \equiv |\zeta\bar{\zeta}\xi\bar{\xi}\bar{\eta}| \\ &|\zeta\beta\rangle \equiv |\xi\bar{\xi}\eta\bar{\eta}\bar{\zeta}| && |\zeta\alpha\rangle \equiv |\xi\bar{\xi}\eta\bar{\eta}\zeta| \end{aligned} \tag{11}$$

$$\xi \equiv d_{yz}; \qquad \eta \equiv d_{xz}; \qquad \zeta \equiv d_{xy} \tag{11a}$$

The wave functions of the iron(III) porphyrin complex could be now composed in the following manner. The ground state will be

$$\begin{aligned} \mathrm{G}^+ &= |a_1\bar{a}_1a_2\bar{a}_2 + | \equiv a|a_1\bar{a}_1a_2\bar{a}_2\zeta\bar{\zeta}\eta\bar{\eta}\xi| - ib|a_1\bar{a}_1a_2\bar{a}_2\zeta\bar{\zeta}\xi\bar{\xi}\eta| - c|a_1\bar{a}_1a_2\bar{a}_2\xi\bar{\xi}\eta\bar{\eta}\bar{\zeta}| \\ \mathrm{G}^- &= |a_1\bar{a}_1a_2\bar{a}_2 - | \equiv -a|a_1\bar{a}_1a_2\bar{a}_2\zeta\bar{\zeta}\eta\bar{\eta}\bar{\xi}| - ib|a_1\bar{a}_1a_2\bar{a}_2\zeta\bar{\zeta}\xi\bar{\xi}\bar{\eta}| - c|a_1\bar{a}_1a_2\bar{a}_2\xi\bar{\xi}\eta\bar{\eta}\zeta| \end{aligned} \tag{12}$$

The excited configurations B and Q of Eq. (8) become

$$\begin{aligned} \mathrm{B}_x^{\pm} &= \{\sin\theta(|a_1\bar{e}_ya_2\bar{a}_2 \pm | - |\bar{a}_1e_ya_2\bar{a}_2 \pm |) \\ &\qquad + \cos\theta(|a_1\bar{a}_1a_2\bar{e}_x \pm | - |a_1\bar{a}_1\bar{a}_2e_x \pm |)\}/\sqrt{2} \\ \mathrm{B}_y^{\pm} &= \{\sin\theta(|a_1\bar{e}_xa_2\bar{a}_2 \pm | - |\bar{a}_1e_xa_2\bar{a}_2 \pm |) \\ &\qquad - \cos\theta(|a_1\bar{a}_1a_2\bar{e}_y \pm | - |a_1\bar{a}_1\bar{a}_2e_y \pm |)\}/\sqrt{2} \\ \mathrm{Q}_x^{\pm} &= \{\cos\theta(|a_1\bar{e}_ya_2\bar{a}_2 \pm | - |\bar{a}_1e_ya_2\bar{a}_2 \pm |) \\ &\qquad - \sin\theta(|a_1\bar{a}_1a_2\bar{e}_x \pm | - |a_1\bar{a}_1\bar{a}_2e_x \pm |)\}/\sqrt{2} \\ \mathrm{Q}_y^{\pm} &= \{\cos\theta(|a_1\bar{e}_xa_2\bar{a}_2 \pm | - |\bar{a}_1e_xa_2\bar{a}_2 \pm |) \\ &\qquad + \sin\theta(|a_1\bar{a}_1a_2\bar{e}_y \pm | - |a_1\bar{a}_1\bar{a}_2e_y \pm |)\}/\sqrt{2} \end{aligned} \tag{13}$$

Subscripts u and g are omitted.

It should be noted here that a more accurate procedure would require to consider a covalent mixing of π- and d-orbitals. But as will be shown a one-electron mixing would not affect our principal conclusion. In any case one-electron spin orbitals in Slater determinants of Eq. (13) may be considered as the mixed ones. On the other hand, the two-electron interaction between porphyrin and iron orbitals could play a significant role. If so, the electron repulsion operator matrix on a basis set of B- and Q-functions of Eq. (13) must be diagonalized to find the new wavefunctions. The matrix factors into B- and Q-submatrices

$$\begin{array}{c|cc} & \mathrm{B}_x^{\pm} & \mathrm{B}_y^{\pm} \\ \hline \mathrm{B}_x^{\pm} & V_B & \pm iab(S-T\sin 2\theta) \\ \mathrm{B}_y^{\pm} & \mp iab(S-T\sin 2\theta) & V_B \end{array} \tag{14}$$

$$\begin{array}{c|cc} & \mathrm{Q}_x^{\pm} & \mathrm{Q}_y^{\pm} \\ \hline \mathrm{Q}_x^{\pm} & V_Q & \pm iab(S+T\sin 2\theta) \\ \mathrm{Q}_y^{\pm} & \mp iab(S+T\sin 2\theta) & V_Q \end{array} \tag{15}$$

where

$$S \equiv \{\langle e_x\xi|e^2/r_{12}|\eta e_y\rangle - \langle e_x\eta|e^2/r_{12}|\xi e_y\rangle\}/2 \tag{16}$$

$$T \equiv \langle a_2\xi|e^2/r_{12}|\eta a_1\rangle \tag{17}$$

New energy levels will be

$$E_{1,2}(\mathrm{B}) = V_B \pm ab(S-T\sin 2\theta) \tag{18}$$

$$E_{1,2}(\mathrm{Q}) = V_Q \pm ab(S+T\sin 2\theta) \tag{19}$$

and the corresponding wave functions are given by

$$\begin{aligned} \mathrm{B}_1^{\pm} &= (\mathrm{B}_x^{\pm} \mp i\mathrm{B}_y^{\pm})/\sqrt{2} \\ \mathrm{B}_2^{\pm} &= (\mathrm{B}_x^{\pm} \pm i\mathrm{B}_y^{\pm})/\sqrt{2} \\ \mathrm{Q}_1^{\pm} &= (\mathrm{Q}_x^{\pm} \mp i\mathrm{Q}_y^{\pm})/\sqrt{2} \\ \mathrm{Q}_2^{\pm} &= (\mathrm{Q}_x^{\pm} \pm i\mathrm{Q}_y^{\pm})/\sqrt{2} \end{aligned} \tag{20}$$

To calculate the MCD parameters for $\mathrm{G}^{\pm} \rightarrow \mathrm{Q}_{1,2}^{\pm}$ and $\mathrm{B}_{1,2}^{\pm}$ transitions one may use the general formulae by Stephens *et al.* [1]

$$\begin{aligned} A(a \rightarrow j) &= (2d_a)^{-1} \sum [\langle j|\boldsymbol{\mu}|j\rangle - \langle a|\boldsymbol{\mu}|a\rangle] \operatorname{Im} [\langle a|\boldsymbol{m}|j\rangle \times \langle j|\boldsymbol{m}|a\rangle] \\ C(a \rightarrow j) &= (2d_a)^{-1} \sum \langle a|\boldsymbol{\mu}|a\rangle \operatorname{Im} [\langle a|\boldsymbol{\mu}|j\rangle \times \langle j|\boldsymbol{m}|a\rangle] \end{aligned} \tag{21}$$

where d_a is the degeneracy of a, and $\boldsymbol{m}$ and $\boldsymbol{\mu}$ are the electric- and magnetic-dipole operators, respectively. The summations are over all transitions degenerate with $a \rightarrow j$.

We neglect here the B-terms, which may arise due to B–Q mixing in the presence of a magnetic field. There are discrepancies in literature on this subject as McHugh *et al.* [12] pointed out. As to B-terms owing to Q_1–Q_2- and B_1–B_2-mixings, they are forbidden.

To get information on the temperature behaviour of MCD it is convenient to calculate the relative C/A values. Substituting wave functions given by Eqs. (12), (13) and (20) for a and j of Eq. (21) we can obtain the C/A ratios shown in Table 1.

Table 1. The relative values of MCD parameters calculated for isolated components of orbit–orbit split Q and B bands (+ and − refer to different components (see text))

Band	C/A
Q	$\pm\dfrac{(a+b)^2-c^2}{\langle e_y\vert\mu_z\vert e_x\rangle+\sin 2\theta\langle a_1\vert\mu_z\vert a_2\rangle}$
B	$\pm\dfrac{(a+b)^2-c^2}{\langle e_y\vert\mu_z\vert e_x\rangle-\sin 2\theta\langle a_1\vert\mu_z\vert a_2\rangle}$

The expected MCD dispersion curves could be obtained by using the following relation connecting molecular parameters of Eq. (21) with experimentally observed MCD ($\Delta A_M = A_L - A_R$), provided magnetic moments, electric moments, energies and magnetic field are expressed in bohr magnetons, debye units, cm^{-1} and Tesla, respectively:

$$\frac{\Delta A_M}{\mathrm{C}\cdot\mathrm{l}\cdot\mathrm{H}} \equiv \Delta\varepsilon_M = 64.7\sum_i\left[\frac{\partial f(\nu_i,\nu,\Gamma)}{\partial\nu_i}\cdot A_i - f(\nu_i,\nu,\Gamma)\cdot\frac{C_i}{T}\right] \tag{22}$$

where subscripts i refer to any given $a\rightarrow j$ transition, f defines absorption band shape, concentration C and pathlength l are expressed in mole litre^{-1} and in cm, respectively.

Again the picture similar to Fig. 3 appears, since the denominator of the C/A-ratios for $\mathrm{G}^{\pm}\rightarrow\mathrm{Q}^{\pm}_{1,2}$ transitions are larger than those for $\mathrm{G}^{\pm}\rightarrow\mathrm{B}^{\pm}_{1,2}$ ones (see Table 1).

It should be noted that the results of the present section correlate with those of the preceding by the following substitutions [13]:

$$\begin{aligned}(\eta\pm i\xi)/\sqrt{2}&=|\pm1\rangle\\(a_2\pm ia_1)/\sqrt{2}&=|\pm4\rangle\\(e_x\pm ie_y)/\sqrt{2}&=|\pm5\rangle\end{aligned} \tag{23}$$

i.e. when $\theta=\pi/4$ and $a=b=1/2$, $c=0$ (pure tetragonal environment). Then the energy splittings of Eqs. (18, 19) transform into ΔB and ΔQ of Eq. (5). But unlike with ring wave functions, where the radial part was simply equal to $\delta(r-R)$-function, the radial dependences of porphyrin orbitals are much more complex. Consequently the signs of parameters S and T of Eqs. (16, 17) are not predictable *a priori*, as it was possible for the signs of ΔQ and ΔB provided Hund's rule had been valid. Perhaps just for this reason the sign of MCD of the myoglobin CN^- complex, observed in the Q band by Springall *et al.* [6] at liquid helium temperature, is opposite to the room temperature sign.

4. Discussion

To verify our model we have measured the low-temperature MCD of the deoxymyoglobin NO complex (Fig. 4). The 2.1-fold increase of peak-to-peak intensity in low temperature Soret MCD is much greater than the increase expectable for the *A*-type effect owing to a 1.15-fold enhancement of the absorption amplitude. Therefore we may speak about the *C*-type effects in the B band.

The NO ground state is known to be $^2\Pi$ and one may expect the spin–orbit coupled Kramers doublet as in the case of the inner circular ring with odd numbers of electrons considered above. Thus the same theoretical arguments as for iron(III) low-spin heme could in principle be applied, providing the π(porphyrin)–π(NO) interaction is sufficiently appreciable. At the same time the low-spin ferrous state

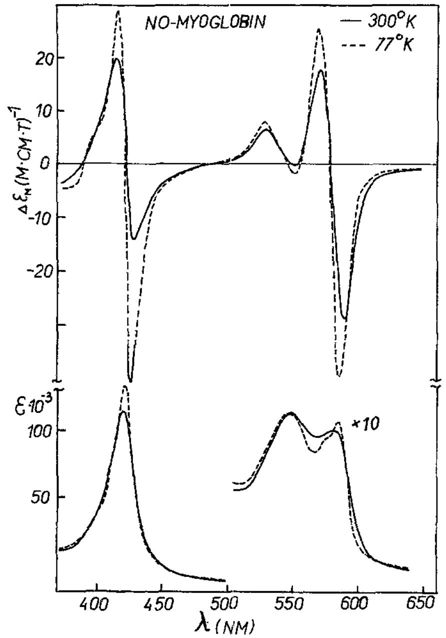

Fig. 4. Magnetic circular dichroism and absorption spectra of nitrosyl complex of Fe(II)-myoglobin at room (——) and liquid nitrogen (- - -) temperatures. Protein concentration $1.4\cdot 10^{-4}$ M in near UV and $1.4\cdot 10^{-3}$ M in the visible; in an equal-volume mixture of glycerol amd 0.2 M bis-tris buffer at pH 6.8; pathlength 0.5 mm; magnetic field 1.56 T

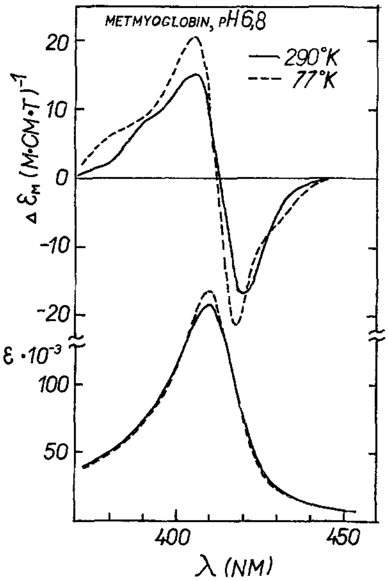

Fig. 5. Magnetic circular dichroism and absorption spectra of metmyoglobin at room (——) and liquid nitrogen (- - -) temperatures. Protein concentration $1.4\cdot 10^{-4}$ M; in an equal-volume mixture of glycerol and 0.2 M bis-tris buffer at pH 6.8; pathlength 0.5 mm; magnetic field 1.56 T

of heme in NO-myoglobin excludes the possibility of charge transfer transition (4 → 1) by Kobayashi *et al.* [4].

As to the interpretation implying appreciable spin(iron)–orbit(porphyrin) coupling by Livshitz *et al.* [3], we believe that such an interaction certainly takes place in paramagnetic iron–porphyrin complexes. However it seems to be much less than the exchange-type one. This statement is confirmed by experiments by Gale *et al.* [14], who have measured the MCD spectra of Cu(II)-porphyrin down to 8°K and no *C*-type effects have been found in spite of the presence of the unpaired $d_{x^2-y^2}$-electron.

Additional experimental evidence on this question is presented here. In Fig. 5 the low-temperature MCD of metmyoglobin ($S=5/2$) is shown. The slight increase of MCD intensities at liquid nitrogen temperature could be surely attributed to that of absorption intensities (see bottom panel of Fig. 5). On the other hand, according to Livshitz *et al.*'s model, one might expect the significant *C*-type effects just in this compound since all possible 3*d*-orbitals contain an unpaired electron.

If our model is valid, one could ask how it is possible to get experimentally the parameters of the orbit–orbit interaction. The procedure is similar to that described in Ref. [3], where the ΔB-value has been obtained by comparing *C*-terms of MCD and absorption band. In terms of our consideration this means that the $ab(S \pm T \sin 2\theta)$-values of Eqs. (18, 19) could be determined in principle from absorption and MCD after room and low-temperature measurements. Then one can obtain the net parameters S and T, provided a, b and $\sin 2\theta$ are known from independent experiments. However, the assignments of g-factors from EPR studies are somewhat ambiguous, and hence the determination of a, b and c meets some difficulties [11]. At the same time $\sin 2\theta$ could be found only from the absorption spectrum [8], which in turn is broadened due to the excited-state splittings. All these reasons complicated experimental evaluations of S and T parameters. The overcoming of these difficulties invites further studies.

Acknowledgements. We are grateful to Dr. N. A. Sharonova and Mr. V. A. Figlovsky for their help and to Dr. M. A. Livshitz for helpful discussions. We thank Dr. W. R. Melyk-Adamyan and Dr. V. V. Barynin for a sample of beef-liver catalase. We wish to acknowledge Prof. M. V. Volkenstein for his encouragement.

References

1. Stephens, P. J.: Ann. Rev. Phys. Chem. **25**, 201 (1974)
2. Briat, B., Berger, D., Leliboux, M.: J. Chem. Phys. **57**, 5606 (1972)

3a. Livshitz, M. A., Arutyunyan, A. M., Sharonov, Yu. A.: Dokl. Acad. Nauk USSR **223**, 487 (1975)
3b. Livshitz, M. A., Arutyunyan, A. M., Sharonov, Yu. A.: J. Chem. Phys. **64**, 1276 (1976)
4. Kobayashi, H., Higuchi, T., Eguchi, K.: Bull. Chem. Soc. Japan **49**, 457 (1976)
5a. Vickery, L., Nozawa, T., Sauer, K.: J. Am. Chem. Soc. **98**, 343 (1976)
5b. Vickery, L., Nozawa, T., Sauer, K.: J. Am. Chem. Soc. **98**, 351 (1976)
6. Springall, J., Stillman, M. J., Thomson, A. Z.: Biochim. Biophys. Acta **453**, 494 (1976)
7. Serber, R.: Phys. Rev. **41**, 489 (1932)

8. Gouterman, M.: J. Chem. Phys. **30**, 1139 (1959)
9. Dratz, E. A.: Ph.D. Thesis, University of California, Berkeley [Radiation Lab. Report UCRL-17200] (1966)
10. Simpson, W. T.: J. Chem. Phys. **17**, 1218 (1949)
11. Taylor, C. P. S.: Biochim. Biophys. Acta **491**, 137 (1977)
12. McHugh, A. J., Gouterman, M., Weiss, C.: Theoret. Chim. Acta (Berl.) **24**, 346 (1972)
13. Gouterman, M.: J. Chem. Phys. **33**, 1523 (1960)
14. Gale, R., McCaffrey, A. J., Rowe, M. D.: J. Chem. Soc. Dalton **5**, 596 (1972)

Received February 17, 1978